

Research Note

# Breaking the dispersion-reducibility dependence in oxide-supported cobalt nanoparticles

Agustín Martínez\*, Gonzalo Prieto

*Instituto de Tecnología Química, UPV-CSIC, Avda. de los Naranjos s/n, 46022 Valencia, Spain*

Received 16 August 2006; revised 31 October 2006; accepted 2 November 2006

Available online 28 November 2006

## Abstract

Cobalt metal nanoparticles ca. 4–5 nm in size synthesized in the core of reverse micelles and supported on surface-protected delaminated ITQ-2 zeolite display a very narrow particle size distribution and a high reducibility typical of larger particles. The methodological preparation approach presented here allows breaking of the dispersion–reducibility dependence inherent to very small cobalt particles supported on oxidic carriers, thereby overcoming long-lasting difficulties in studying particle size effects in highly dispersed cobalt-based Fischer–Tropsch catalysts.

© 2006 Elsevier Inc. All rights reserved.

*Keywords:* Cobalt catalyst; Delaminated zeolite; ITQ-2; Fischer–Tropsch; Reducibility

## 1. Introduction

Fischer–Tropsch (FT) synthesis is an attractive route to produce environmentally friendly fuels and specialties from alternative sources to petroleum, such as natural gas and biomass, via synthesis gas (mixture of CO and H<sub>2</sub>). FT catalysts based on cobalt supported on oxidic carriers (SiO<sub>2</sub>, Al<sub>2</sub>O<sub>3</sub>, and, to a lesser extent, TiO<sub>2</sub>) are preferred over those based on iron for the production of ultra-clean diesel fuels, because they are more active per weight of metal, more selective to long-chain linear paraffins (waxes), and more stable under FT synthesis conditions [1,2]. The FT activity of supported cobalt catalysts is, in principle, proportional to the amount of exposed metallic cobalt atoms. Therefore, increasing the metallic dispersion by decreasing the particle size seems a logical strategy to improve the activity of cobalt-based FT catalysts.

Unfortunately, however, very small cobalt particles in highly dispersed catalysts interact strongly with the surface hydroxyl groups of the oxidic carrier during thermal activation treatments, leading to the formation of mixed oxides (i.e., cobalt silicates in the case of Co/SiO<sub>2</sub> catalysts), which are difficult to reduce and inactive for CO hydrogenation [3–5]. Moreover,

enhanced formation of undesired methane at the expense of the heaviest hydrocarbons is generally observed for catalysts presenting high cobalt dispersion and thus poor reducibility [6–8]. Besides the negative effect on activity and selectivity, the dispersion–reducibility dependence inherent to very small cobalt nanoparticles supported on oxidic carriers imposes serious limitations to the investigation of structure sensitivity effects in FT catalysis, because the co-existence of incompletely reduced cobalt phases and metallic cobalt within the same particle creates ambiguity about the true particle size effects.

It is thus clear that the decrease in particle size in fundamental catalytic studies aimed at addressing particle size effects in FT chemistry must be accomplished without paying a penalty in reducibility. In this respect, although it appears from the work of Iglesia and co-workers [2,9] that the activity per exposed Co<sup>0</sup> site [turnover frequency (TOF)] under typical FT synthesis conditions favoring high C<sub>5+</sub> selectivity is not influenced by cobalt dispersion in the range of 0.5–11%, corresponding to cobalt particle sizes of about 200–9 nm, respectively, the picture becomes less clear for smaller particles. In this sense, both decreased [10,11] and constant [12] TOF values have been reported for supported cobalt particles below the critical size of 8–10 nm. Therefore, assessment of the effects of cobalt particle size in highly dispersed catalysts becomes of paramount importance for designing novel catalysts

\* Corresponding author. Fax: +34 963877808.

E-mail address: [amart@itq.upv.es](mailto:amart@itq.upv.es) (A. Martínez).

with improved FT synthesis performance. In a recent work, Bezemer et al. [13] took a step toward addressing this problem by using inert carbon nanofibers as carriers for dispersing cobalt. However, cobalt catalysts of very small particle sizes (<5 nm) could be obtained only at low cobalt loadings (<5 wt%) owing to the limitations inherent to the conventional preparation methodologies (mostly impregnation) used in that work.

Here we present an attractive approach to preparing well-defined oxide-supported cobalt nanoparticles with very narrow particle size distribution and high reducibility. By using the proposed preparation methodology, the size of the supported cobalt nanoparticles can be finely tuned at cobalt loadings that are relevant from a practical standpoint. The approach basically comprises the *ex-carrier* synthesis of cobalt nanoparticles in the core of reverse micelles and their subsequent deposition on a surface-protected delaminated all-silica ITQ-2 zeolite. Synthesis of nanoparticles by the reverse microemulsion method allows a fine control of particle size with a very narrow size distribution, whereas protection of the ITQ-2 surface by silylation before cobalt deposition avoids the formation of barely reducible cobalt species. Moreover, the unique textural properties of the delaminated ITQ-2 material presenting an exceptionally large external surface area (>800 m<sup>2</sup>/g) makes this material ideal for accepting the bulky micelles containing the cobalt nanoparticles, thus maintaining high dispersions even at relatively high cobalt loadings.

## 2. Experimental

The all-silica ITQ-2 zeolite was synthesized by swelling the interlaminar space of the layered all-silica MWW precursor and forcing the layers apart by ultrasonication, as reported previously [14]. Silylation of the ITQ-2 surface was achieved by reacting the outgassed calcined solid with a solution of 1,1,1,3,3,3-hexamethyldisilazane (Aldrich, 97%) in toluene under nitrogen atmosphere.

Cobalt nanoparticles were synthesized in a reverse microemulsion using the nonionic surfactant Triton X114 (Acros), *n*-hexanol as the organic phase, and isopropanol as a cosurfactant. The cobalt concentration in the aqueous core of the micelles was 0.3 M using Co(NO<sub>3</sub>)<sub>2</sub>·6H<sub>2</sub>O (Aldrich, 98%) as precursor, and the water-to-surfactant molar ratio was set to 6. Formation of cobalt nanoparticles in the core of the micelles was achieved after addition of hydrazine monohydrate (Aldrich, 98%) to the stable microemulsion. Then the silylated ITQ-2 and the microemulsion were slurried in the required proportions to achieve a nominal cobalt loading of 10 wt%. Subsequently, tetrahydrofuran (THF) was slowly added to destabilize the micellar medium, forcing the cobalt nanoparticles to deposit on the external surface of the zeolitic layers, as schematically presented in Fig. 1. Finally, the solid was decanted, vacuum-filtered, exhaustively washed with ethanol, dried at room temperature overnight and at 333 K for 10 h, and finally calcined at 773 K for 3 h in flowing air to remove the remaining surfac-

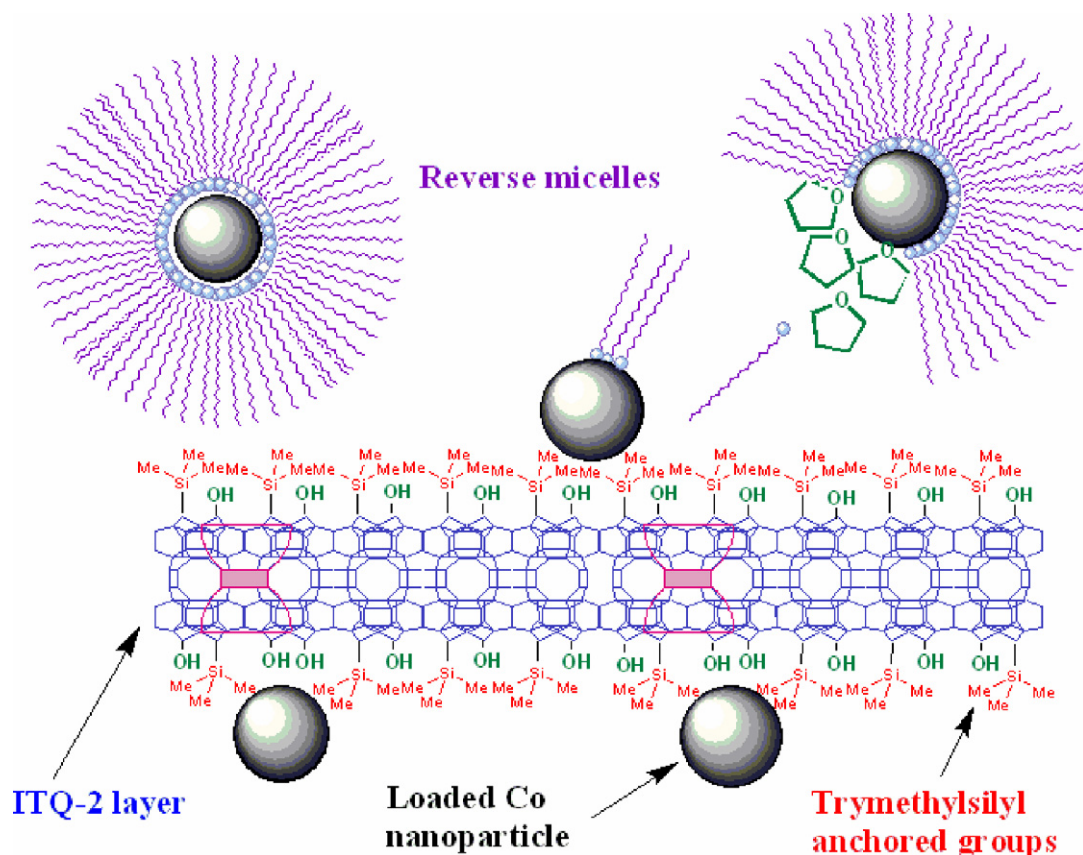


Fig. 1. Schematic representation of the preparation of sample Co\_ME\_S by deposition of cobalt nanoparticles synthesized *ex-carrier* by reverse microemulsion on the silylated ITQ-2 zeolite.

tant and the anchored trimethylsilyl groups. The carbon content in the calcined material was  $<0.4$  wt%, as determined by elemental analysis. The catalyst prepared in this way was denoted as Co\_ME\_S. To better appraise the advantages of this approach, three additional samples were prepared, one of them by depositing the cobalt nanoparticles synthesized in the same microemulsion described above on a nonsilylated ITQ-2 sample (Co\_ME), and the other two by incipient wetness impregnation of either silylated (Co\_IM\_S) or nonsilylated (Co\_IM) ITQ-2 with an ethanolic solution of cobalt nitrate. In all cases the nominal cobalt loading was 10 wt%.

The cobalt loading in the final catalysts was determined by atomic absorption spectrophotometry (AAS) in a Varian Spectra A-10 Plus apparatus. X-ray diffraction (XRD) patterns of calcined samples were obtained in a Philips X'Pert diffractometer using monochromatized  $\text{CuK}\alpha$  radiation.

The BET surface areas of the untreated and silylated ITQ-2 were derived from the corresponding nitrogen adsorption isotherms determined at 77 K in a Micromeritics ASAP 2000 device. Before the adsorption measurements, the samples were outgassed at 473 K for 24 h.

$^{29}\text{Si}$  magic-angle spinning (MAS) nuclear magnetic resonance (NMR) spectroscopy was used to study the silylation of the ITQ-2 surface before cobalt deposition. The spectra were recorded with a Bruker AV400 spectrometer using a 7-mm probe at a spinning rate of 5 kHz.

Transmission electron microscopy (TEM) was used to determine the size of the cobalt particles synthesized in reverse micelles. For unloaded particles, an aliquot volume of the microemulsion containing the cobalt nanoparticles was extracted and deposited on a carbon-covered copper grid (300 mesh); then a THF drop was added to destabilize the micellar medium, and the grid was washed with ethanol and then let to dry. The supported catalysts were previously reduced at 673 K for 10 h in flowing  $\text{H}_2$ . Then a portion of grounded solid was suspended in  $\text{CH}_2\text{Cl}_2$  and sonicated for 1 min. Finally, a drop was extracted under sonication, deposited on the copper grid, and allowed to dry before observation. The nature of the cobalt phases present in Co\_ME\_S sample was studied by selected area electron diffraction (SAED) obtained at five different locations throughout the TEM grid to check for homogeneity.

The reduction behavior of the supported oxidized cobalt phases was studied by hydrogen temperature-programmed reduction ( $\text{H}_2$ -TPR) in a Micromeritics Autochem 2910 device. About 30 mg of the calcined catalyst were initially flushed with  $30\text{ cm}^3/\text{min}$  of Ar at room temperature for 30 min, after which a mixture of 10 vol% of  $\text{H}_2$  in Ar was passed through the catalyst at a total flow rate of  $50\text{ cm}^3/\text{min}$  while the temperature was increased up to 1173 K at a heating rate of 10 K/min. The  $\text{H}_2$  consumption rate was monitored in a thermal conductivity detector (TCD) previously calibrated using the reduction of CuO as a reference.

Hydrogen temperature-programmed desorption ( $\text{H}_2$ -TPD) experiments were performed in the same equipment to estimate the metallic dispersion in selected samples. About 100 mg of the calcined sample were reduced using a flow of high-purity hydrogen ( $100\text{ cm}^3/\text{min}$ , purity  $>99.999\%$ ) at 723 K for 10 h

(heating rate of 1 K/min). The sample was then cooled to 303 K in flowing  $\text{H}_2$  ( $5\text{ K}/\text{min}$ ). The catalyst was held at 303 K for 1 h under flowing Ar to remove physisorbed species, after which the temperature was increased up to the applied reduction temperature (723 K) in flowing Ar ( $10\text{ cm}^3/\text{min}$ ) to desorb chemisorbed hydrogen. The desorbed hydrogen was monitored in a TCD coupled with a mass spectrometer. The cobalt metal particle size was estimated from the amount of chemisorbed hydrogen assuming spherical geometry for the particles and an adsorption stoichiometry of  $\text{H}:\text{Co}_s = 1$ .

The catalysts prepared by microemulsion and by impregnation on silylated ITQ-2 (Co\_ME\_S and Co\_IM\_S, respectively) were tested for FT synthesis in a downflow fixed-bed stainless steel reactor. Before the catalytic experiments, the catalysts were reduced in situ at atmospheric pressure by increasing the temperature at a rate of 1 K/min from ambient up to 723 K and maintained at this temperature for 10 h while passing a flow of pure hydrogen through the reactor. The following reaction conditions were used:  $T = 493\text{ K}$ ,  $P = 2.0\text{ MPa}$ , and  $\text{H}_2/\text{CO}$  molar ratio of 2. The space velocity was varied to obtain CO conversions  $<10\%$ . The intrinsic activity (TOF) was calculated as the number of CO molecules converted per surface Co atoms per second considering the  $\text{Co}^0$  dispersion obtained by  $\text{H}_2$  chemisorption. No correction of the TOF values accounting for the extent of reduction of the samples at 723 K for 10 h was done, because the reducibility of the cobalt precursors in the studied catalysts was seen to be very high, as deduced from  $\text{H}_2$ -TPR. A more detailed description of the experimental setup used for the catalytic study has been given previously [8].

### 3. Results and discussion

The calcined ITQ-2 sample displayed a BET surface area of  $964\text{ m}^2/\text{g}$  and negligible microporosity, as expected from its layered structure. A slightly lower BET value ( $877\text{ m}^2/\text{g}$ ) was obtained for the silylated ITQ-2 material. Silylation of the ITQ-2 carrier was followed by  $^{29}\text{Si}$  MAS NMR spectroscopy. The spectra of the untreated and the silylated samples are presented in Fig. 2. Both samples show bands in the range of  $-90$  to  $-120$  ppm, corresponding to different Si environments in the zeolite structure. The presence of an additional band at  $+13.9$  ppm attributed to silicon atoms in the trimethylsilyl groups in the spectrum of the silylated sample and the 5.13 wt% carbon content in this sample determined by elemental analysis confirmed the silylation of the ITQ-2 surface. The broad signal in the  $-90$  to  $-120$  ppm range could be decomposed into five individual components, as shown in the decomposed spectrum of the nonsilylated sample (insert in Fig. 2). The signals at about  $-105$ ,  $-110$ , and  $-119$  ppm are assigned to  $\text{Q}^4\text{Si}$  species [ $\text{Si}-(\text{O}-\text{Si})_4$ ] in distinct crystallographic positions of the MWW structure, the band at ca.  $-101$  ppm is attributed to  $\text{Q}^3\text{Si}$  or single hydroxyl groups [ $\text{OH}-\text{Si}-(\text{O}-\text{Si})_3$ ], and the band at  $-92$  ppm is assigned to  $\text{Q}^2\text{Si}$  or geminal hydroxyl groups [ $(\text{OH})_2-\text{Si}-(\text{O}-\text{Si})_2$ ] [16]. As expected, the % area under the decomposed curves (not shown) in the spectra of the two samples, excluding the band at  $+13.9$  ppm in the silylated sample, revealed a decrease in the relative concentration of  $\text{Q}^3$  and  $\text{Q}^2$

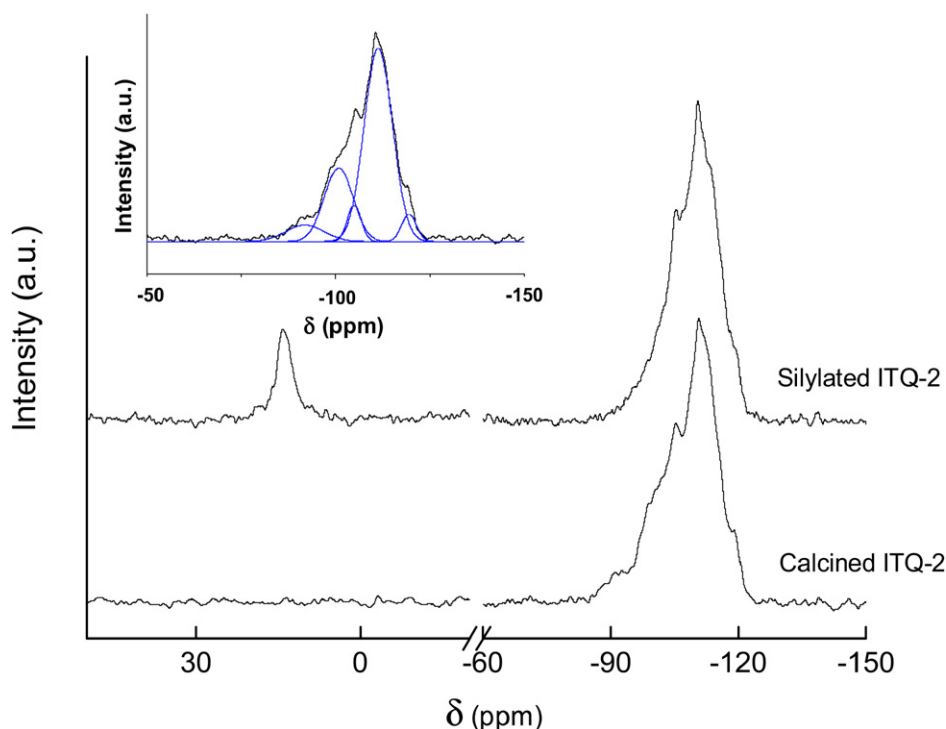


Fig. 2.  $^{29}\text{Si}$  MAS NMR spectra for the non-silylated and silylated ITQ-2 zeolite. The insert shows the spectrum for the non-silylated sample decomposed into five components corresponding to  $\text{Q}^4\text{Si}$  ( $-105$ ,  $-110$ , and  $-119$  ppm),  $\text{Q}^3\text{Si}$  (ca.  $-101$  ppm), and  $\text{Q}^2\text{Si}$  ( $-92$  ppm) species.

Table 1

Average cobalt particle sizes and dispersions obtained from XRD, TEM, and  $\text{H}_2$ -TPD measurements for the different Co/ITQ-2 samples

Sample	XRD			TEM		$\text{H}_2$ -TPD	
	$d(\text{Co}_3\text{O}_4)$ (nm)	$d(\text{Co}^0)$ (nm)	$D(\text{Co}^0)$ (%)	$d(\text{Co}^0)$ (nm)	$D(\text{Co}^0)$ (%)	$\text{H}_2$ uptake ( $\mu\text{mol}/\text{g}_{\text{cat}}$ )	$d(\text{Co}^0)$ (nm)
Co_IM	7.6	5.7	16.8	–	–	–	–
Co_IM_S	11.8	8.9	10.8	9.9[4.2] <sup>a</sup>	9.7	75	10.9
Co_ME	5.6	4.2	22.9	–	–	–	–
Co_ME_S	5.8	4.4	21.8	4.6[0.8] <sup>a</sup>	20.9	199	4.1

<sup>a</sup> Values in brackets are the standard deviations ( $\sigma$ ) obtained for the size distributions given in Fig. 4.

groups on silylation. The extent of silylation (ES, in %) and the specific surface coverage ( $\alpha_S$ , in anchored groups/ $\text{nm}^2$ ) were estimated from the following equations:

$$\text{ES} = \frac{[A_{\text{Q}^2} + A_{\text{Q}^3}]_{\text{non-silylated}} - [A_{\text{Q}^2} + A_{\text{Q}^3}]_{\text{silylated}}}{[A_{\text{Q}^2} + A_{\text{Q}^3}]_{\text{non-silylated}}} \times 100 (\%),$$

$$\alpha_S = \frac{(\Delta C/100) \times N_A}{12 \times 3 \times A \times 10^{18}} \text{ (anchored groups}/\text{nm}^2\text{)},$$

where  $A_i$  is the % area of the  $^{29}\text{Si}$  NMR band corresponding to the  $i$ -type of silicon atoms,  $\Delta C$  is the change in carbon content (in wt%) on silylation,  $A$  is the BET surface area of the original sample (in  $\text{m}^2/\text{g}$ ), and  $N_A$  is Avogadro's number. The results show values of 40% and 1.22 groups/ $\text{nm}^2$  for ES and  $\alpha_S$ , respectively, which are within the range of values given in the literature for silylated siliceous solids [15,16].

The cobalt content in the calcined catalysts was very close to the expected nominal content of 10 wt%. The spinel  $\text{Co}_3\text{O}_4$  was the only crystalline cobalt phase detected by XRD in the calcined samples (not shown). The mean particle sizes of the

supported  $\text{Co}_3\text{O}_4$  phase estimated by XRD from the most intense reflection at  $2\theta = 36.7^\circ$  using Scherrer's equation are given in Table 1. This table also gives the corresponding metallic cobalt particle sizes,  $d(\text{Co}^0)$ , obtained by considering the relative molar volumes of  $\text{Co}^0$  and  $\text{Co}_3\text{O}_4$  [17], and the metal cobalt dispersions,  $D(\text{Co}^0)$ , estimated from  $d(\text{Co}^0)$  assuming a spherical geometry of the metal particles with uniform site density of 14.6 atoms per  $\text{nm}^2$ . It can be clearly seen from the table that the mean  $\text{Co}^0$  particle sizes in the samples prepared by microemulsion are almost identical ( $\sim 4.5$  nm) irrespective of the nature of the ITQ-2 surface (i.e., silylated or nonsilylated). This is not the case, however, when the cobalt is deposited on the ITQ-2 surface by impregnation. In that case, significantly larger particles are formed on the silylated support due to sintering during calcination induced by a weaker interaction of cobalt with the silylated ITQ-2 surface.

TEM was performed after reduction at 673 K for 10 h in flowing  $\text{H}_2$  for the samples containing the silylated zeolite. Fig. 3 shows representative TEM images for the sample prepared by the *ex-carrier* synthesis of cobalt nanoparticles

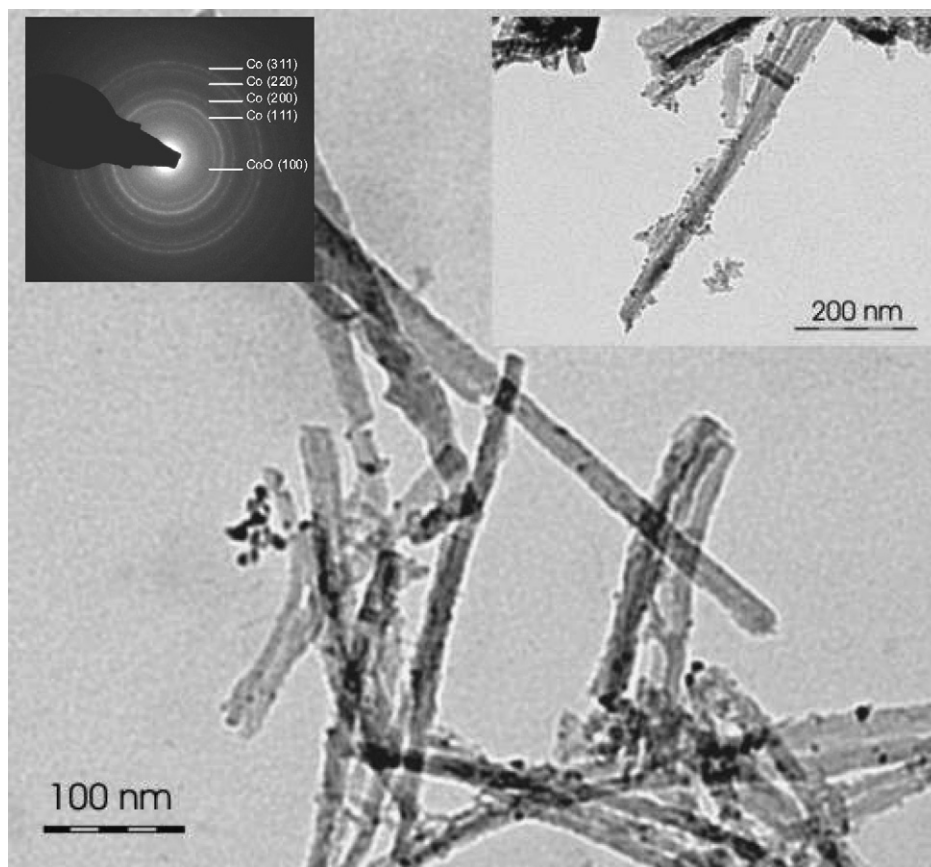


Fig. 3. Representative TEM micrographs for Co\_ME\_S catalyst pre-reduced at 723 K for 10 h showing the cobalt nanoparticles of about 4–5 nm diameter as black spots on the ITQ-2 layers. The selected area electron diffraction (SAED) pattern of this sample is also shown in the top left side insert.

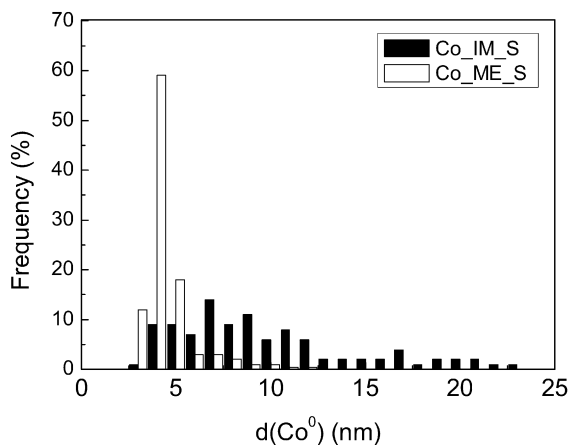


Fig. 4. Cobalt particle size distributions derived from representative TEM images for pre-reduced (723 K for 10 h) Co\_ME\_S and Co\_IM\_S samples.

(Co\_ME\_S). The images clearly reveal the layered nature of the ITQ-2 material and the presence of cobalt particles of about 4–5 nm in diameter as black spots on the layers. Remarkably, the cobalt particles are very homogeneous in size, thereby discarding any extensive sintering during the reduction treatment at 673 K. Moreover, the singular structure of ITQ-2 lacking significant intraparticle porosity allows direct observation of the cobalt particles by TEM, which is a very valuable feature for fundamental studies, because it increases the reliability of

the particle size determination by this technique. In fact, ambiguous determination of the particle size is, in many cases, in the origin of uncertainties when calculating TOF values in Co-based FT catalysts [11,18]. As seen in Table 1, the average cobalt particle sizes derived from TEM are in complete agreement with those estimated by XRD. On the other hand, the particle size histograms obtained from TEM for the samples comprising the silylated zeolite as support reveal a narrower cobalt particle size distribution for the catalyst prepared by the reverse micellar method compared with that obtained by impregnation (Fig. 4). We note here that some surface reoxidation of the cobalt nanoparticles occurred during sample preparation before TEM observation, as evidenced by the SAED characterization on the better dispersed Co\_ME\_S sample. Thus, a representative diffraction pattern is shown as an insert in Fig. 3 (top left side), displaying concentric rings assigned to randomly oriented Co<sup>0</sup> (fcc) nanoparticles together with a weak diffraction ring due to *d*-spacing of ca. 0.214 nm ascribed to the most intense diffraction line of (200) in cubic CoO [19]. Nevertheless, the presence of the surface CoO phase would modify the size from a completely reduced particle in less than 15% considering the relative molar volumes of Co<sup>0</sup> and CoO phases, which is within the standard deviation ( $\sigma$ ) for the particle size distribution (Table 1). As seen in Table 1, the mean Co<sup>0</sup> particle sizes for Co\_ME\_S and Co\_IM\_S samples estimated from H<sub>2</sub> chemisorption measurements are 4.1 and 10.9 nm, respectively,

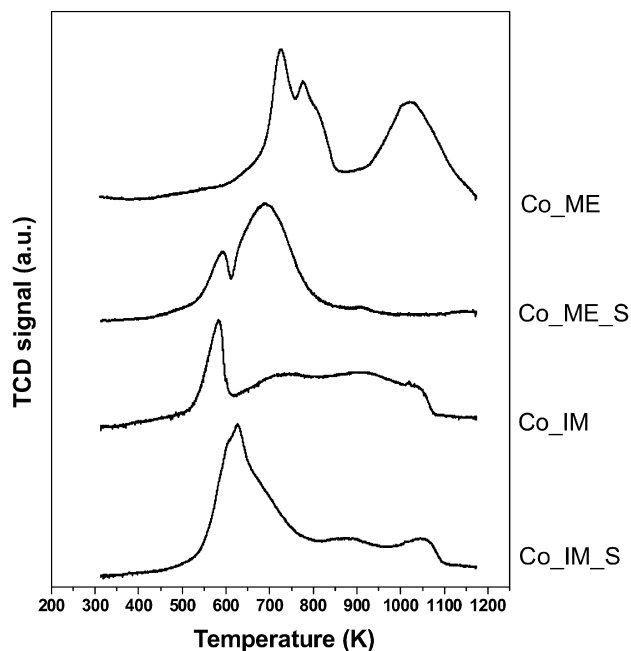


Fig. 5.  $H_2$ -TPR profiles for the different Co/ITQ-2 catalysts. Note the almost absence of high temperature ( $>800$  K) reduction peaks in the Co\_ME\_S sample prepared according to the proposed methodology.

which are in good agreement with those derived from XRD and TEM.

In addition, the reduction behavior of the supported cobalt catalysts was studied by  $H_2$ -TPR. The reduction profiles for the different catalysts prepared are presented in Fig. 5. As would be expected from its larger cobalt particle size (Table 1), the sample prepared by impregnation of silylated ITQ-2 (Co\_IM\_S) displays good reducibility, although it still presents some reduction features at temperatures above 800 K, probably ascribed to small cobalt particles interacting more strongly with the support. Interestingly, deposition of cobalt particles synthesized *ex-carrier* by microemulsion on the silylated ITQ-2 almost suppresses the formation of cobalt species which are difficult to reduce, as evidenced from the absence of significant reduction features above 800 K in the reduction profile of sample Co\_ME\_S. The benefit of silylation of the ITQ-2 surface on cobalt reducibility is further supported by the presence of an intense reduction feature peaking at about 1025 K in the nonsilylated Co\_ME sample, indicating the formation of cobalt silicates during the activation treatment. Therefore, protecting the surface OH groups of ITQ-2 by silylation before the deposition of cobalt nanoparticles is essential to avoid the formation of barely reducible mixed oxides, allowing achievement of high reduction degrees at the typical reduction temperatures applied for Co-based FT catalysts. To the best of our knowledge, the preparation methodology reported here is a pioneering approach to attaining cobalt nanoparticles supported on oxidic carriers as small as 4–5 nm at relatively high cobalt loading and displaying a reducibility behavior hitherto exclusive to fairly larger particles.

The intrinsic activity for the FT synthesis at 493 K of the very small cobalt nanoparticles present in Co\_ME\_S having an

average particle size of 4.1 nm (derived from  $H_2$  chemisorption) was seen to be much lower ( $TOF = 0.3 \times 10^{-3} s^{-1}$ ) than that of the larger cobalt particles (ca. 11 nm) in the impregnated Co\_IM\_S sample ( $TOF = 28.5 \times 10^{-3} s^{-1}$ ). It must be stated that the TOF of the impregnated catalyst stems from the contribution of cobalt particles of quite different sizes, according to the broad particle size distribution inherent to this preparation method (Fig. 4). The TOF was seen to increase from  $0.3 \times 10^{-3}$  to  $1.3 \times 10^{-3} s^{-1}$  when the mean diameter of the cobalt nanoparticles was increased from 4.1 to 5.8 nm in samples prepared according to the new approach proposed here. These preliminary results point out to a drastic decrease in the TOF value when the size of the supported cobalt particles is decreased to  $<10$  nm and are in line with previous works for cobalt catalysts supported on amorphous silica [11] and carbon nanofibers [13].

#### 4. Conclusion

In summary, we have shown that the combination of using a surface-silylated delaminated ITQ-2 zeolite as support with the *ex-carrier* synthesis of nanoparticles by reverse microemulsion allows for the preparation of very small ( $\sim 4$ –5 nm) supported cobalt particles displaying a narrow particle size distribution and high reducibility. This new approach may offer an attractive alternative for tackling fundamental catalytic studies, such as structure sensitivity effects in FT catalysis, without being disturbed by reducibility limitations. Furthermore, the model catalyst system presented here can also be extended to study the influence of promoters in bimetallic FT catalysts (e.g., Co–Ru) by isolating the true promoting effect from the effects associated to changes in dispersion and/or reducibility induced by the presence of the promoter.

#### Acknowledgments

Financial support by the Comisión Interministerial de Ciencia y Tecnología (CICYT) of Spain through the Project CTQ 2004-02510/PPQ is gratefully acknowledged. The authors thank Dr. A. Vidal-Moya and Prof. V. Fornés for performing the NMR and  $H_2$ -TPD measurements. G. Prieto thanks the Ministerio de Educación y Ciencia (MEC) of Spain for a Ph.D. scholarship.

#### References

- [1] M.E. Dry, Catal. Today 6 (1990) 183.
- [2] E. Iglesia, Appl. Catal. A 161 (1997) 59.
- [3] B. Sexton, A. Hughes, T. Turney, J. Catal. 97 (1986) 390.
- [4] B. Ernst, S. Libs, P. Chaumette, A. Kiennermann, Appl. Catal. A 186 (1999) 145.
- [5] A.M. Saib, M. Claeys, E. van Steen, Catal. Today 71 (2002) 395.
- [6] R.C. Reuel, C.H. Bartholomew, J. Catal. 85 (1984) 78.
- [7] A.Y. Khodakov, A. Groboval-Constant, R. Bechara, V.L. Zholobenko, J. Catal. 206 (2002) 230.
- [8] A. Martínez, C. López, F. Márquez, I. Díaz, J. Catal. 220 (2003) 486.
- [9] E. Iglesia, S.L. Soled, R.A. Fiato, J. Catal. 137 (1992) 212.
- [10] A.S. Lisitsyn, A.V. Golovin, V.L. Kuznetsov, Yu.I. Yermakov, J. Catal. 95 (1985) 527.

- [11] A. Barbier, A. Tuel, I. Arcon, A. Kodre, G.A. Marin, *J. Catal.* 200 (2001) 106.
- [12] S.-W. Ho, M. Houalla, D.M. Hercules, *J. Phys. Chem.* 94 (1990) 6396.
- [13] G.L. Bezemer, J.H. Bitter, H.P.C.E. Kuipers, H. Oosterbeek, J.E. Holewijn, X. Xu, F. Kapteijn, A.J. van Dillen, K.P. de Jong, *J. Am. Chem. Soc.* 128 (2006) 3956.
- [14] A. Corma, V. Fornés, S.B. Pergher, Th.L.M. Maesen, J.G. Buglass, *Nature* 396 (1998) 353.
- [15] X.S. Zhao, G.Q. Lu, A.K. Whitaker, G.J. Millar, H.Y. Zhu, *J. Phys. Chem. B* 101 (1997) 6525.
- [16] X.S. Zhao, G.Q. Lu, *J. Phys. Chem. B* 102 (1998) 1556.
- [17] D. Schanke, S. Vada, E.A. Blekkan, A.M. Hilmen, A. Hoff, A. Holmen, *J. Catal.* 156 (1995) 85.
- [18] A.M. Saib, A. Borgna, J. van de Loosdrecht, P.J. van Berge, J.W. Geus, J.W. Niemantsverdriet, *J. Catal.* 239 (2006) 326.
- [19] S.G. Oh, R.T.K. Baker, *J. Catal.* 128 (1991) 137.